

# **A New Method for Event Detection and Location - Matched Field Processing Application to the Salton Sea Geothermal Field\***

**Jingbo Wang<sup>1</sup>, Dennise Templeton<sup>1</sup>, and Dave Harris<sup>2</sup>**

Search and Discovery Article #40946 (2012)

Posted June 18, 2012

\*Adapted from extended abstract prepared in conjunction with oral presentation at AAPG Annual Convention and Exhibition, Long Beach, California, April 22-25, 2012, AAPG©2012

<sup>1</sup>Lawrence Livermore National Lab, Livermore, CA, United States ([jbw\\_cam@hotmail.com](mailto:jbw_cam@hotmail.com))

<sup>2</sup>Deschutes Signal Processing, LLC, Maupin, OR, United States.

## **Abstract**

We apply the empirical matched field processing (MFP) method to continuous seismic data to detect and locate more microearthquakes than can be detected using only conventional earthquake detection techniques. We demonstrate that empirical MFP can complement existing catalogs and techniques by increasing earthquake catalog completeness. The empirical MFP method finds events in the continuous data stream by identifying signals that match pre-defined master templates. We identify and construct representative master templates using the Southern California Earthquake Data Center (SCEDC) earthquake catalog and continuous waveform data of events originating within the Salton Sea Geothermal Field study area. We identify 231 master templates that have good quality data at four or more seismic stations. We apply the empirical MFP method to continuous seismic data collected at the Salton Sea Geothermal Field between November 2009 and December 2010. The MFP method successfully identified 6496 local events, while the original catalog only reported 1536 events. We empirically determine the magnitude of these new events and can clearly show that the completeness magnitude,  $M_c$ , the magnitude above which all earthquakes are considered to be detected by a seismic network, was lowered when using the existing seismic station and just adding the MFP algorithm to the standard data processing. It clearly shows that many smaller earthquakes with magnitudes between 0 and 1 were added to the catalog. Therefore, we believe that the empirical MFP method, when combined with conventional methods, significantly improves network detection capabilities.

## **Introduction**

Accurate identification and mapping of large numbers of microearthquakes is one technique that provides diagnostic information when determining the location, orientation and length of underground crack systems. Conventional earthquake location techniques are often employed to locate microearthquakes. These techniques require accurate picking of individual seismic phase onsets across a network of sensors and work best on seismic records containing a single well-recorded event with high signal-to-noise ratio. Seismic phase picking, however, can become difficult or impossible on seismic records containing large numbers of overlapping events or events with poor signal-to-noise ratios.

To aid in the seismic characterization of reservoir fracture networks, we complement traditional earthquake detection and location techniques with the empirical matched field processing (MFP) method. The empirical MFP method matches the spatial structure of incoming seismicity observed by a network of sensors to master templates keyed to potential event locations. Empirical MFP steers the array by summing signals observed over a network using complex phase and amplitude weights obtained from existing event templates (Harris and Kvaerna, 2010). This is different from the conventional seismic array processing method, delay-and-sum beamforming, which steers an array by applying time delays to align waveforms recorded by array elements. Empirical MFP is different from traditional waveform correlation techniques because it decomposes the signal into many narrow frequency bands and treats each as independent quantities. This is done in order to suppress the dependence on source time function, which is inherent in traditional waveform correlation techniques.

Empirical MFP develops a catalog of matching templates from a collection of representative microearthquakes that densely sample the study volume. The earthquakes for the empirical master templates are initially located using conventional earthquake location techniques, and subsequently relocated using advanced processing techniques, however all future seismicity is mapped using the computationally efficient MFP algorithm. In this article, we apply this technique to continuous seismic data, which includes two earthquake swarms, collected in the Salton Sea Geothermal Field between November 2009 and December 2010 to demonstrate the power of the increased detection capability of empirical MFP.

## **Study Area**

The Salton Sea Geothermal Field (SSGF) is located in Southern California at the southern end of the Salton Sea within the Salton Trough, an active tectonic pull-apart basin. A portion of the SSGF is situated within the Brawley Seismic Zone, which extends across the Salton Sea to connect with the San Andreas Fault to the north and the Imperial Fault to the south (Fuis and Mooney, 1990). This zone is the most northerly of a series of spreading centers, distributed along the length of the Salton Trough and within the Gulf of California that can be associated with the East Pacific Rise. Rifting and intrusions produce high heat flow that metamorphoses the

sedimentary rocks to shallow depths (Fuis et al., 1984).

A local surface seismic monitoring network, the EN network, monitors SSGF seismic activity. The EN network is composed of eight three-component seismic stations (Figure 1). The instruments are 4.5 Hz L15B three-component geophones. Since January 2008, continuous data from this network has been archived at the Southern California Earthquake Data Center (SCEDC). The data during this time period includes two of the largest seismic swarms that occurred in the SSGF since continuous seismic data has been archived at the SCEDC.

## Method

Our MFP technique is an adaptation of a signal processing technique originally developed to locate continuous underwater acoustic sources (Bucker 1976; Baggeroer et al. 1993). We calculate the wavefield structure across an array by estimating the structure directly from previous seismic events. The master templates, therefore, contain contributions from both direct and scattered seismic energy. We refer to this strategy as empirical MFP.

Empirical MFP breaks the signals into a large number of narrow frequency bands, chooses processing parameters that make signals in the narrow bands approximately independent, performs the matching operation band by band, and combines the results incoherently across bands. The independence of the signal in the narrow bands helps to reduce the complication made by the source time history of the events (Harris and Kvaerna, 2010). When performing the matching operation, we develop a steering vector calibration for the network of seismic stations in each narrow frequency band for each potential source location defined by the master events. This vector of complex weight can be calculated as the principal eigenvector of the covariance matrix estimated from each master template.

Our detection methodology can be described in 5 steps (Figure 2). The first step is to obtain the locations and waveforms of the catalog events. The second step is to determine which events should be chosen as field calibration events. Waveforms of calibration events must have high signal-to-noise ratios. The records must also be free of additional seismic events within a specified time window that spans both before and after the actual microearthquake signal. Step 3 is to run the empirical MFP code on one day of continuous seismic data from all available seismic channels to identify events in the data stream that can match to the master templates. In the fourth step we verify that energy can be detected between 8-40 Hz to exclude matches between low-frequency noise in templates and continuous data. Finally, we visually verify all new detections and compare to catalog events.

## Event Locations and Waveforms

For the event locations, we have both the original hypoinverse solutions from the SCEDC catalog and the waveform cross-correlation

relocation results by Hauksson et al. (2012). As the catalog of Hauksson et al. (2012) provides a better relative location of the events by performing the waveform cross-correlation, we plot all events using the locations from the Hauksson et al. (2012) catalog. There are 2977 catalog events by Hauksson et al. (2012) during January 2008 to December 2010 within a 10 km radius centered at seismic station HAT (Figure 1).

Continuous seismic data from the EN network was downloaded from the SCEDC website. The sample rate of the continuous data is 100 samples per second (SPS).

### **Master Events Selection**

Theoretically, as more master templates are located throughout the study volume, we would be able to identify more new events. Therefore, we visually inspected the waveforms of all events between 2008 and 2010 that were in the original SCEDC catalog and identified those with the best quality data. These events have little noise, especially in the lower frequency ranges, and do not have significant seismic events within a 70 sec time window that includes the proposed master event. The master events must also include at least four stations with good quality recordings. We identify 231 master events out of the original 2977 catalog events (Figure 1).

In general, the background noise is incoherent across the 70 sec time window at stations ELM, ENG, HAT, OBS, RED, and YOU. However, station LIN displays a higher background noise level than the other stations. Therefore, we decided to remove station LIN from the processing due to its poor quality of recording. The other stations do not consistently display high background noise energy.

### **Run Empirical MFP**

The empirical MFP code performs its calculation on the continuous data using a 70-sec window which steps forward 1 second at a time. Figure 3 shows a 10-day example of results for the time period January 11-20, 2010. This segment of data is band-pass filtered between 4-10 Hz. The y-value at each time point indicates the normalized detection statistic. A value of 1 would indicate an exact match between the template and the incoming seismicity at that particular time. Threshold levels for each detector are calculated over each 1-day period and are a function of the average detection statistic value. Detection statistics above the threshold are compared to detections at other detectors. If multiple detectors identify the same event, the detector with the largest detection statistic is then determined to have detected the event. The two detectors in Figure 3 show representative behavior.

As illustrated in Figure 3, Detector 157 (origin time: 2010/01/13, 14:14:30) shows an elevated detection statistic around January 15. Detector 157 is able to correctly identify itself with a detection statistic of 1 at the appropriate time. Detector 1 (origin time: 2008/01/21, 03:29:28) has a totally different detection pattern from Detector 157 and detected very few events. An investigation into

the relative location of these detectors shows that Detector 157 is located in the middle of the January 15 earthquake swarm while Detector 1 is located on the fringe of the seismicity. This illustrates the fact that the more spatially evenly sampled the master events are, the higher chance we will have to be able to detect more events within the study volume.

### **Spectrogram Check**

The automatic spectrogram check identifies whether a proposed detection is a real event by checking the strength of the signals in the 8-40 Hz range. We calculate a function based on the ratio between the energy around the arrival time of the proposed event to the pre-event energy. If the function is above a certain threshold at over half of the channels, the proposed event is ruled to be a real event. After a thorough study, we verified that this procedure delivers similar results to a manual inspection on the proposed detections.

### **Visual Inspection and Catalog Check**

The final step is to visually check the detections claimed by the spectrogram check and to exclude nearby regional events that fall outside our study area, but produced a signal across the local network. These nearby events are excluded by comparing the timing of the new events with the regional earthquake catalog.

## **MFP Results and Discussion**

For this study, we applied the empirical MFP method to continuous data collected between November 2009 and December 2010. We compared 231 master templates to the data stream and identified 6496 local events. The Hauksson et al. (2012) catalog reported 1536 events and the SCEDC catalog reported 1562 events over the same period (Figure 4). Therefore, we believe that our method demonstrates that MFP is a powerful tool to help identify more events than those identified using conventional event detection methods.

Figure 4 shows the impact of the nearby and extremely large 4 April 2010 Mw 7.2 El Mayor-Cucapah earthquake and aftershock sequence across our network. The fault rupture extended 75 km northwest, from the epicenter in Baja California through the US-Mexico border (<http://www.scsn.org>). More than 4000 aftershocks occurred afterwards, including 5 earthquakes greater than magnitude 6. Due to the close distance between the ruptured fault area and our study area, many aftershocks were recorded by the EN network. These events are easily excluded by comparing the potential detection list with the regional earthquake catalog.

We also reconcile the local catalog of events with our results. Our method found 306 of the 333 catalog events reported in the Hauksson et al. (2012) catalog during January 2010. There are 8.1% catalog events still missing. This is likely due to a lack of full

coverage of the master templates of the seismogenic region (see [Figure 1](#)). Therefore, some events near the region where no master templates located might be missed in our empirical MFP method. However, with more and more data available as time goes on, we expect to have a full coverage over the whole region eventually.

### **Magnitude of the New Events**

We also investigate the magnitude of the new events in our study. Firstly, we define the SNR of the signal using:

$$\text{SNR} = \frac{\text{Amplitude of signal}}{\text{Amplitude of noise}}$$

We obtain the amplitude of the signal by stacking the P-wave energy over all available vertical components. We determine the amplitude of noise by averaging the absolute value over 2-second window right before the event origin time. In [Figure 5](#), a regression line was drawn to obtain the empirical relationship in our region between the magnitude and  $\log_{10}$  (SNR) of the catalog events. The newly detected events not reported by the Hauksson et al. (2012) catalog, are plotted along the regression line to obtain an estimated magnitude based on the above empirical relationship.

A histogram of events detected by both the Hauksson et al. (2012) catalog and the MFP method is plotted in [Figure 6](#). The new events detected only by the MFP method are plotted in red and the catalog events are in blue. It is clear that the MFP method greatly increases the catalog completeness of the smaller magnitude events.

### **Conclusions**

MFP with empirically calibrated master templates is able to detect more events than can be detected using only conventional earthquake detection techniques. Unlike most array processing methods, empirical MFP does not require a plane wave assumption. Therefore, empirical MFP is more flexible in noisy environments, as long as the master templates adequately cover the area where future events will possibly occur. Our test on SSGF continuous data between November 2009 and December 2010 demonstrates the detection capability using the empirical MFP method. There are 6496 local events detected in total by the MFP method within the 4-10 Hz frequency band, while the catalog reports only 1536 events. Thus the empirical MFP algorithm significantly improves seismic array detection capability. Finally, we estimate the magnitude of the new events identified by the MFP method. The result shows that most of the new events are low amplitude events with magnitudes between 0 and 1, which clearly demonstrates the improvement of the MFP method on the completeness magnitude of the seismic network.

## Acknowledgements

This work was performed under the auspices of the U.S. Department of Energy by Lawrence Livermore National Laboratory under contract ED-AC52-07NA27344. This work is funded by the American Recovery and Reinvestment Act, Pub. L. 111-5. We thank Robert Mellors, William Walter and Sean Ford for their helpful discussions and comments to improve this manuscript. LLNL contribution number: 564752

## References

- Allis, R., J.N. Moore, J. McCulloch, S. Petty, and T. DeRocher, 2000, Karaha-Telaga Bodas, Indonesia: A Partially Vapor Dominated Geothermal System: Geothermal Resources Council Transactions, v. 24, p. 217-222.
- Baggeroer, A.B., W.A. Kuperman, and P.N. Mikhalevsky, 1993, An overview of matched field methods in ocean acoustics, IEEE Journal of Oceanic Engineering, v. 18/4, p. 401-424.
- Bucker, H.P., 1976, Use of calculated sound fields and matched field detection to locate sound sources in shallow water: Journal of the Acoustical Society of America, v. 59/2, p. 368-373.
- Fuis, G.S., W.D. Mooney, J.H. Healy, G.A. McMechan, and W.J. Lutter, 1984, A seismic refraction survey of the Imperial Valley region, California, Journal of Geophysical Research, v. 89, p. 1165-1189.
- Fuis, G.S., and W.D. Mooney, 1990, Lithospheric structure of California along the San Andreas fault system, from seismic and other data, *in* R.E. Wallace (ed.), the San Andreas fault system: USGS Prof. Paper 1515, p. 207-236.
- Gibbons, J. S., M.B. Sørensen, D.B. Harris, and F. Ringdal, 2007, The detection and location of low magnitude earthquakes in northern Norway using multi-channel waveform correlation at regional distances, Physics of The Earth and Planetary Interiors, v. 160/3-4, p. 285-309.
- Harris, B.D., and T. Kvaerna, 2010, Superresolution with seismic arrays using empirical matched field processing: Geophysical Journal International, v. 182, p. 1455-1477.
- Hooland, A.A., 2002, Microearthquake Study of the Salton Sea Geothermal Field, California: Evidence of stress triggering, Idaho National Engineering and Environmental Laboratory, Geosciences Department, Thesis, The University of Texas at El Paso.

Hauksson, E. and W. Yang, and P.M. Shearer, Waveform Relocated Earthquake Catalog for Southern California (1981 to 2011), in submission: Bulletin Seismological Society of America.

Kohler, M., H. Magistrale, and R. Clayton, 2003, Mantle heterogeneities and the SCEC three-dimensional seismic velocity model version 3, Bulletin Seismological Society of America, v. 93, p. 757-774.

Lin, J., and R.S. Stein, 2004, Stress triggering in thrust and subduction earthquakes, and stress interaction between the southern San Andreas and nearby thrust and strike-slip faults, Journal of Geophysical Research., 109, B02303, doi:10.1029/2003JB002607.

Magistrale, H., S. Day, R.W. Clayton, and R. Graves, 2000, The SCEC southern California reference 3D seismic velocity model Version 2, Bulletin Seismological Society of America, v. 90/6B, S65-S76.

Peng, Z., and P. Zhao, 2009, Migration of the Parkfield early aftershock sequence, Nature Geoscience, doi: 10.1038/ngeo697.

Shelly, D.R., G.C. Beroza, S. Ide, and S. Nakamura, 2006, Low-frequency earthquakes in Shikoku, Japan and their relationship to episodic tremor and slip, Nature, v. 442, p. 188-191.

Toda, S., R.S. Stein, K. Richards-Dinger, and S. Bozkurt, 2005, Forecasting the evolution of seismicity in southern California: Animations built on earthquake stress transfer, Journal of Geophysical Research, B05S16, doi:10.1029/2004JB003415.

Waldhauser, F., 2001, HypoDD - A program to compute double-difference hypocenter locations: U.S. Geological Survey Open-File Report, 01-113.

Waldhauser, F., and L.E. William, 2000, A double-difference earthquake location algorithm: Method and application to the northern Hayward fault, California: Bulletin Seismological Society of America, v. 90, p. 1353-1368.

Yang, W., E. Hauksson, and P.M. Shearer, Computing a large refined catalog of focal mechanisms for southern California (1981-2010), manuscript in preparation, 2012.



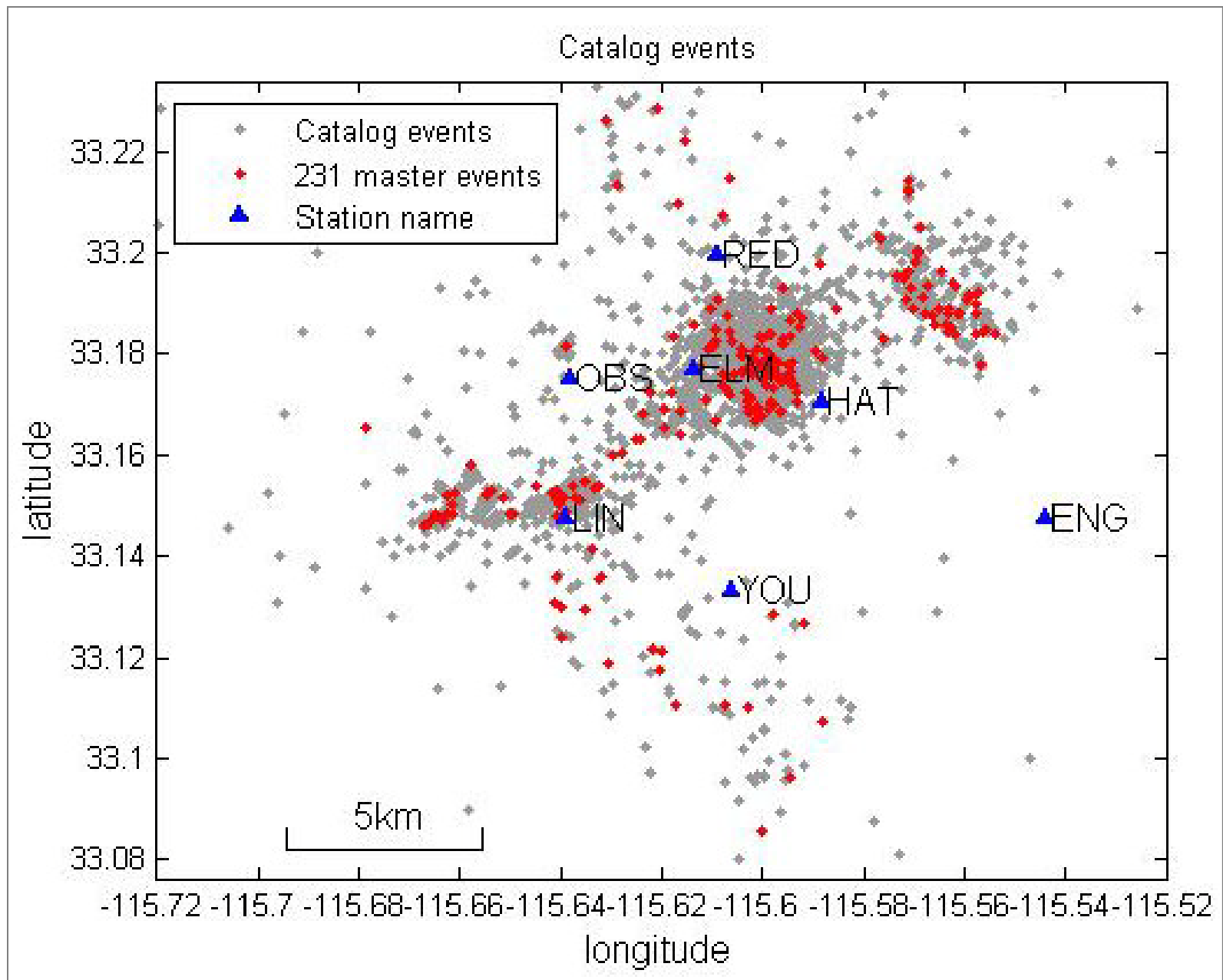


Figure 1. Map view of the seven seismic stations in the EN network which are included in this study. Seismic stations are indicated by blue triangles with station names. The grey dots are catalog events occurring between 2008 and 2010 (Haukson et al., 2012). The master template events are marked in red.

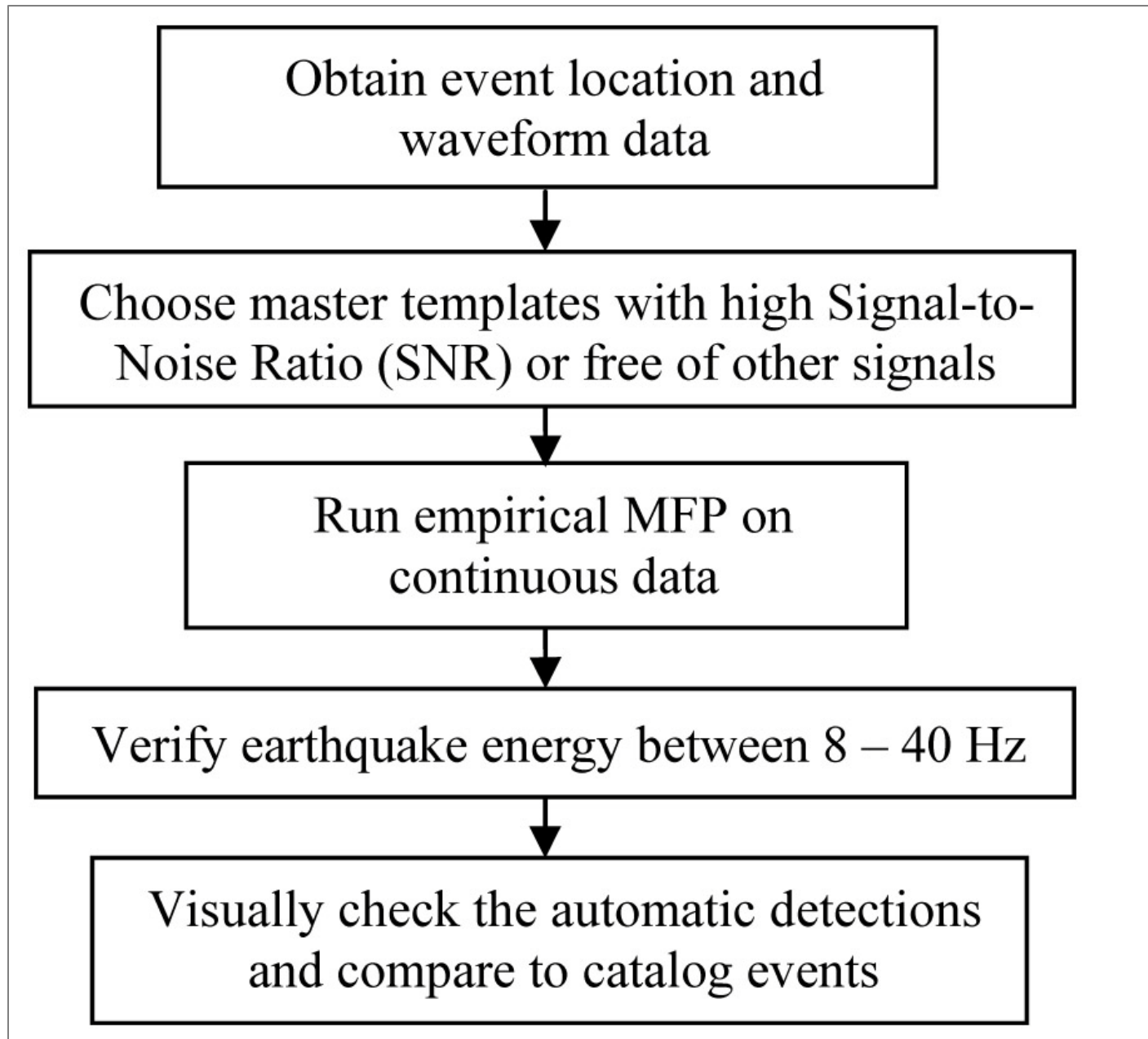


Figure 2. Empirical MFP work flow.

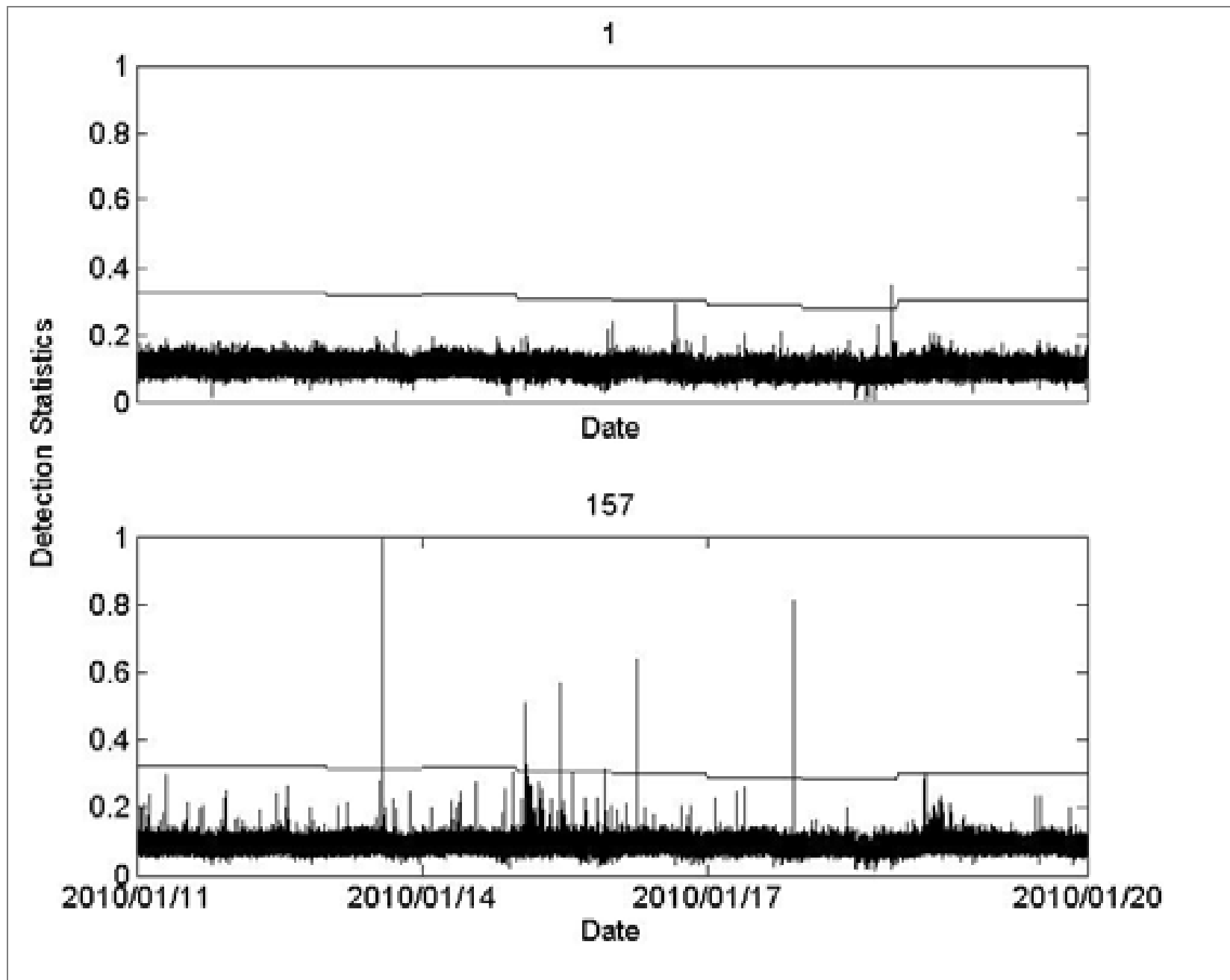


Figure 3. Empirical MFP detection results from two master templates during January 11-20, 2010.

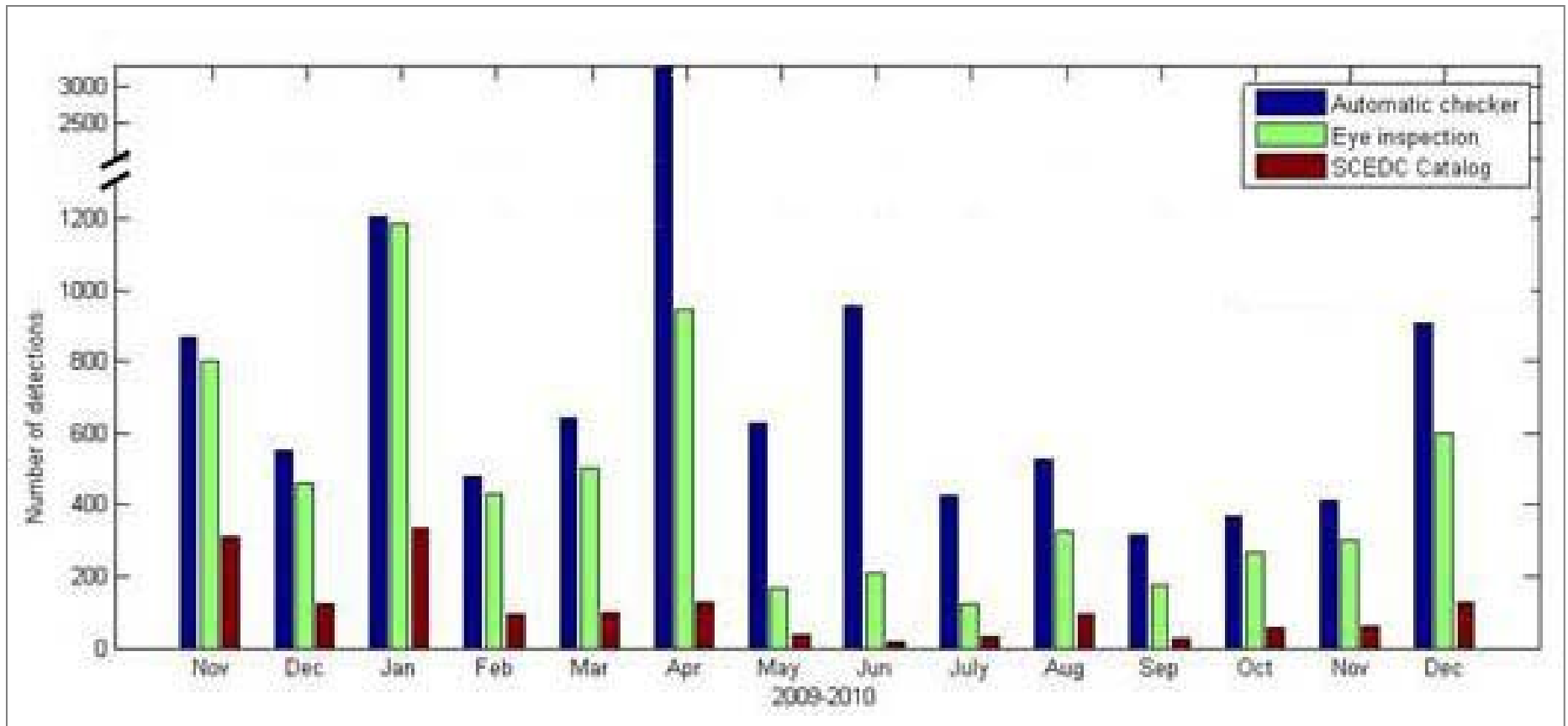


Figure 4. Final results of empirical MFP and comparison to the number of catalog events in the Hauksson et al. (2012).

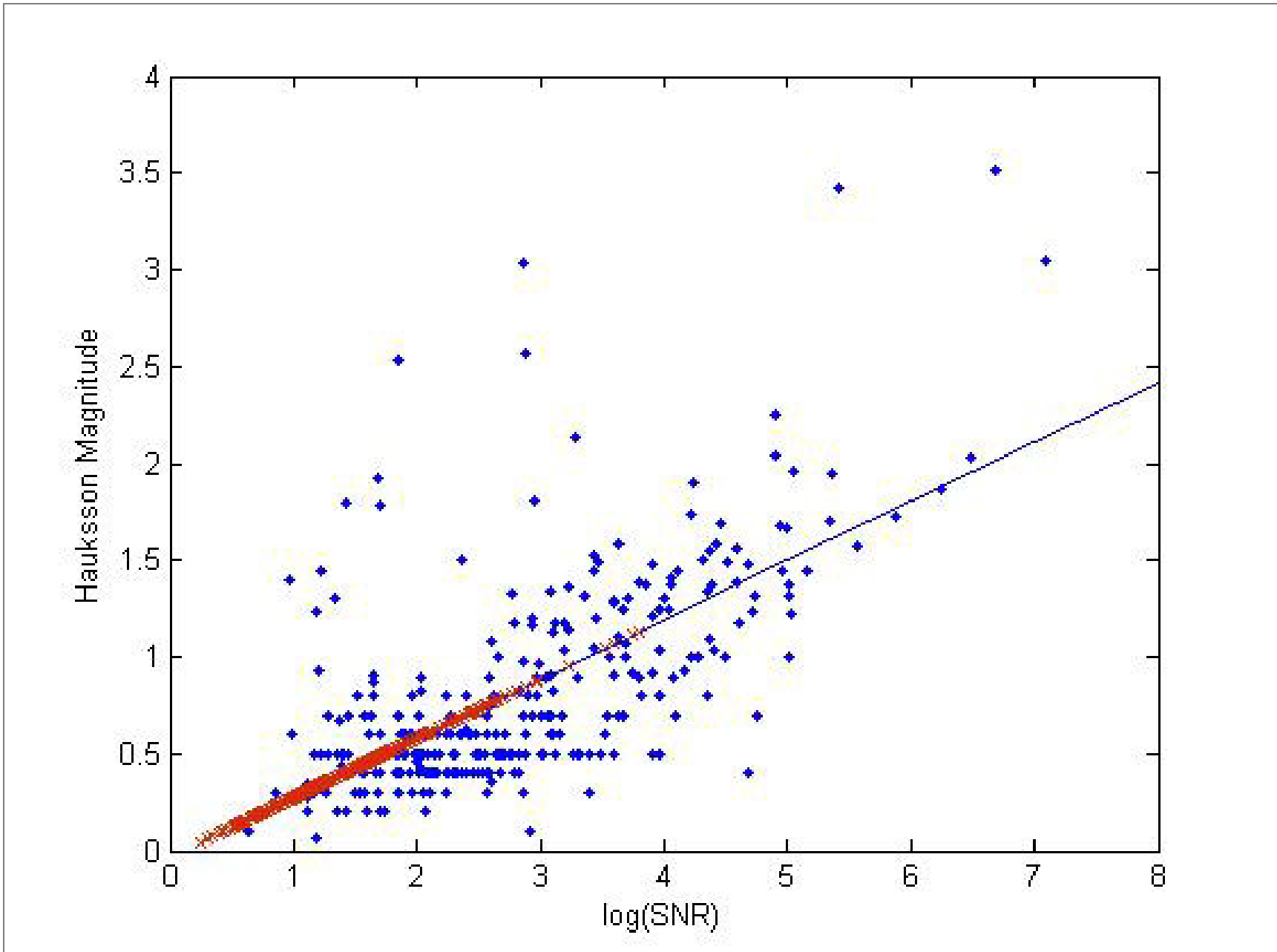


Figure 5. Regression relationship between the magnitude and  $\log_{10}(\text{SNR})$ . The blue dots are the catalog events. The new events are plotted in red along the regression line.

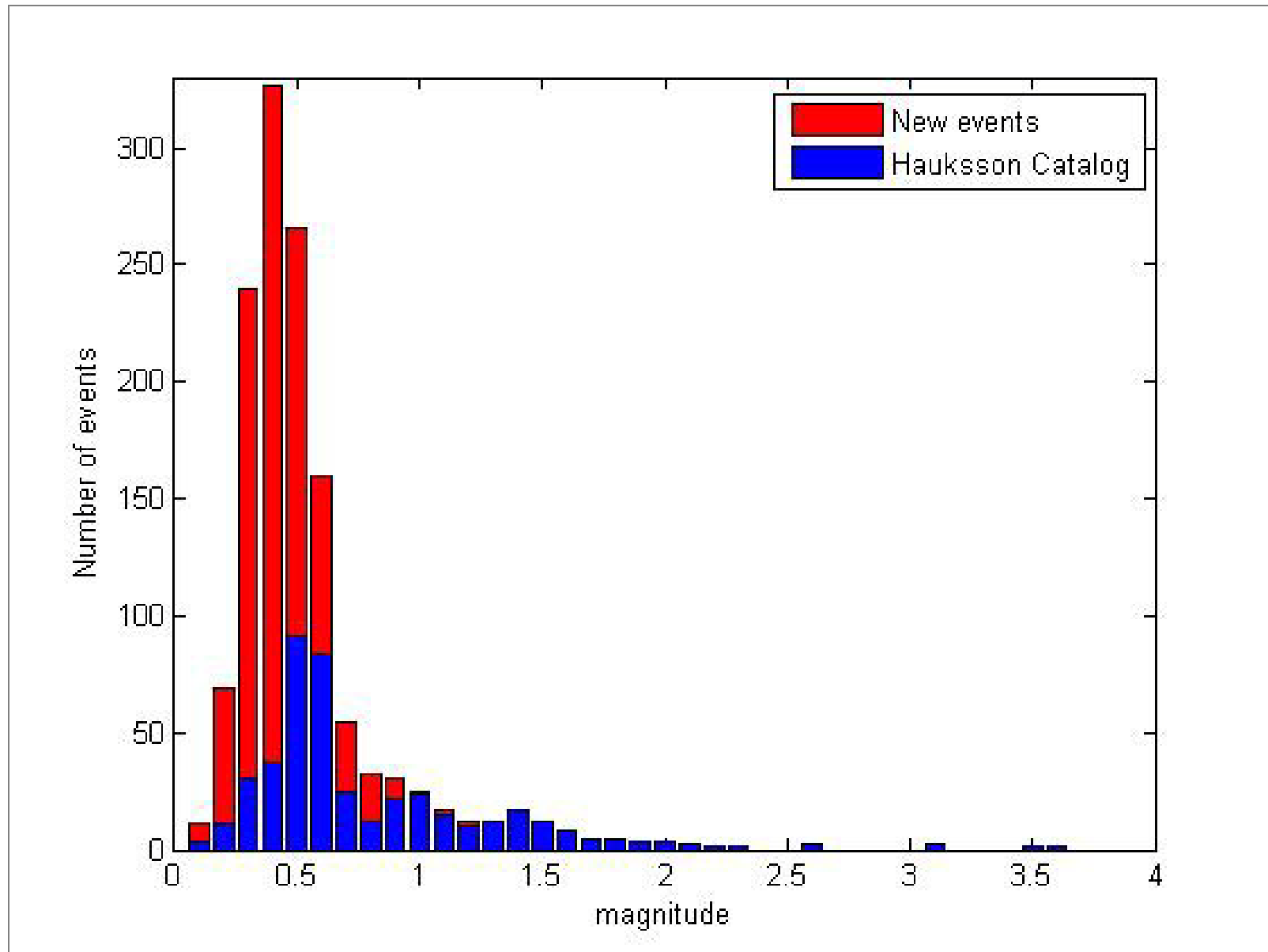


Figure 6. Histogram of the number of events versus the magnitude of the events. The red bars are events detected by the MFP method only. The blue bars are events detected by both MFP and the catalog.